COO-3153-104

23,962

ABSOLUTE LENGTH MEASUREMENT AT HIGH PRESSURE

by

P. C. Lincoln* and Arthur L. Ruoff
Department of Materials Science and Engineering
Cornell University, Ithaca, New York 14850

ABSTRACT

A length measurement system is described which can make absolute length change measurements of a meter long specimen within a pressure vessel (to pressures of 8 kbar) with a fractional error of 3×10^{-8} even when changes in length of 4 cm occur. Possible uses of such a system for measuring the volume thermal expansivity (at pressure) and the isothermal bulk modulus (at pressure) are described. Moreover it is noted that when this system is combined with an ultrasonic velocity measurement system, the adiabatic bulk modulus (at pressure) and Grüneisen parameter as a function of pressure can be directly determined and the absolute pressure itself can be measured.

MASTER

*Now at Sandia Corporation, Albuquerque, New Mexico

DISCLAIMER

INTRODUCTION

Elastically isotropic solids and cubic crystals have a linear compressibility which is isotropic. Therefore the change in length, ℓ, along one direction of such a solid specimen also yields the change in volume, V, since

$$\frac{dV}{V} = \frac{3d\ell}{\ell} . \qquad (1)$$

Thus the isothermal bulk modulus

$$B^T = -V\left(\frac{\partial P}{\partial V}\right)_T = -\frac{\ell}{3}\left(\frac{\partial P}{\partial \ell}\right)_T \qquad (2)$$

can be measured by making length versus pressure, $\ell(P)$, measurements. Similarly the volumetric thermal expansivity at pressure

$$\beta = \frac{1}{V}\left(\frac{\partial V}{\partial T}\right)_P = \frac{3}{\ell}\left(\frac{d\ell}{dT}\right)_P \qquad (3)$$

can be measured by making length versus temperature changes at constant pressure.

If the specific heat at atmospheric pressure is C_P^1, then the specific heat at high pressures C_P can be obtained from the relation[1]

$$C_P = C_P^1 - \int_{P_1}^{P} T\left[\frac{(\partial\beta/\partial T) + \beta^2}{\rho}\right]_P dP . \qquad (4)$$

Here ρ is the density. If the density at atmospheric pressure, ρ_1, is known, then ρ at pressure can be computed from the relation

$$\rho\ell^3 = \rho_1\ell_1^3 . \qquad (5)$$

By combining ultrasonic transit time measurement at pressure with length measurement at the same pressure, the adiabatic bulk modulus

at pressure can be obtained. Thus

$$B^S = \rho \ell^2 \left(\frac{1}{\tau_\ell^2} - \frac{4}{3\tau_\Delta^2}\right). \qquad (6)$$

Here τ_ℓ is the transit time for a longitudinal wave in a [111] direction and τ_Δ is the transit time for a shear wave in the [100] direction.

The thermodynamic Gruneisen parameter is

$$\gamma = \frac{\beta B^S}{\rho C_P} . \qquad (7)$$

Inasmuch as each of these quantities is measured at pressure as previously described, $\gamma(P)$ can be obtained. It is also possible to use the thermodynamic relation

$$B^T = B^S/(1+\Delta) = B^S/1+\beta\gamma T \qquad (8)$$

to obtain γ since B^T, B^S and β can be measured at a particular T and P. The accuracy of this method would not be good if $\beta\gamma T$ were exceptionally small, as for silicon at room temperature. However for materials such as the alkali metals where B^S and B^T differ by several percent (at room temperature) this method is applicable.

Finally, the absolute pressure is given by

$$P = P_1 + 3\rho_1 \ell_1 \int_{\ell_1}^{\ell} \left(\frac{1}{\tau_\ell^2} - \frac{4}{3\tau_\Delta^2}\right) \frac{1}{1+\Delta} \frac{d\ell}{\ell^2} . \qquad (9)$$

The quantity

$$\Delta = \frac{\beta^2 B^S T}{\rho C_P} \qquad (10)$$

can be evaluated as a function of ℓ as previously described, except for C_P where

$$C_P(\ell) = C_P^1 + \int_{\ell_1}^{\ell} 3TB^T \left[\frac{(\partial\beta/\partial T)+\beta^2}{\rho}\right]_\ell d\ell . \qquad (11)$$

Here we note that B^T is contained in the integrand. While B^S can be obtained as a function of ℓ, as in Equation (6), B^T cannot except by an iterative process. If the test specimen is chosen so that Δ is very small, then this iterative process works very well. The use of this system to measure absolute pressure is described elsewhere.[2]

It is clear that a system capable of measuring length at high pressures can be used in many ways. The measurement of length and of length change at pressure is not new. Bridgman made macroscopic length change type equation of state measurements for many solids with the "reference length" inside the pressure vessel.[3] In this case the reference length was a pure iron rod held parallel to the length change specimen and subjected to the same pressure and temperature environment as the specimen. The relative length change measurement was made within the pressure vessel by an electrical slidewire arrangment, with the relative length change magnified by a lever arrangement in some cases. The equation of state of iron was used to calculate the reference length change; hence the results of these experiments are "relative to iron."

Bridgman's equation of state for iron was measured[4] with the pressure vessel wall as the "reference length." The displacement of an axially located iron specimen relative to the inner wall of a pressure vessel was measured with an electrical slidewire. This relative length change measurement was combined with the reference length change as observed by measuring the axial length change of the pressure vessel wall near the outside. The region of the pressure vessel used for the reference length was restricted to

the center of the vessel length to minimize "warping" effects which would invalidate the assumed duplication of inner and outer axial displacements. Rotter and Smith[5] have shown quite conclusively that Bridgman's absolute iron data was in error.

The reference length can be made independent of specimen pressure by locating the reference length outside of the pressure vessel. However the relative length change measurement must be made between a specimen inside the pressure vessel and the reference length outside, requiring some form of displacement coupling through the pressure gradient. Ebert[6] used glass windows in a pressure vessel and marks on the specimen to optically couple displacements through the pressure gradient. Smith et al.[7] used beryllium windows and cast X-ray shadows of V-shaped grooves cut near each end of a specimen. Reitzel et al.[8] used a nonmagnetic stainless steel pressure vessel and observed the displacement of a "magnetic marker" at the end of a specimen with a differential transformer. All of these displacement coupling techniques allow the reference length to be independent of the pressure acting on the specimen, and all of them use some form of micrometer slide or comparator to measure the relative length change.

The present experimental technique is based on four criteria designed to satisfy the requirements of high pressure thermodynamic measurements related to the previously mentioned applications. The design criteria are:

(1) The specimen length change measurement should be absolute, not relative to some other material. Both temperature and pressure dependence of the specimen length should be

measureable and absolute.

(2) The specimen length change measurement error should be less than or equal to $3 \times 10^{-8} \ell_1$, and the specimen initial length measurement error should be less than or equal to $10^{-5} \ell_1$.

(3) The experimental environment should be designed so that materials with linear thermal expansion coefficients as large as 2×10^{-5} cm/cm-°C can be used as specimens.

(4) The specimen environment should be capable of a hydrostatic pressure of 8 kbar, and a temperature range of at least 20°C.

Two kinds of macroscopic reference lengths are available; solid material lengths and optical wavelengths. Both kinds are pressure sensitive; the solid materials have elastic length changes, and optical wavelengths change with index of refraction, which is a function of density, and so changes significantly with pressure for any optically transparent pressure media. Since neither an optical or solid reference length with the required length stability as a function of pressure seems available, the present design has the reference length outside of the pressure vessel. Another experimental part of the $\Delta \ell(T,P)$ measurement is measuring the relative length change between the specimen and reference length. Assuming that the maximum length pressure vessel that one wishes to work with is about 1 meter, and that the maximum specimen length change will be about $.01 \ell_1$ (calculated from $P_{max} \leq 8$ kbar and $B_{min} \geq 300$ kbars), the relative length change measurement must have a span of at least 1 cm with an accuracy equal to or better than 3×10^{-8}

meters (= 300 Å). An optical interferometer has the required accuracy and can be made with a span greater than 1 cm.

DESCRIPTION OF APPARATUS

General

The present system, schematically shown in Figure 1, includes a stabilized laser vacuum wavelength external to the pressure vessel that is used both as a temperature independent reference length and as a standard wavelength for the relative length change measurement interferometer. Displacement coupling through the pressure gradient is accomplished by using magnetic cores inside nonmagnetic "tails" of the pressure vessel (see Figure 2), and nulling on these markers with differential transformers.

A cylindrical specimen with a length between 103 and 109 cm is supported on the axis of a pressure vessel by longitudinal ball bushings. Nonmagnetic extensions of the pressure vessel, made of 316 stainless steel tubing having a 12.7 mm O.D. and a 5.6 mm I.D., are attached to the ends of the pressure vessel. The maraging steel vessel has a 7.6 cm O.D., a 1.75 cm I.D. and a length of 91 cm. The axially centered specimen extends beyond the ends of the pressure vessel approximately seven centimeters into each nonmagnetic tail.

Linear variable differential transformers (LVDT's - Schaevitz Engineering, Camden, New Jersey - Model 030X5-K) at atmospheric pressure surround the tails at each end of the specimen (see Figure 2) and are used to indicate the axial position of the LVDT cores which are spring loaded against each end of the specimen.

Displacement coupling involves translating the ambient pressure LVDT's until the LVDTs are nulled on the core centroids, and repeating this process (for both specimen ends) each time a length change measurement is made.

The core geometry used to minimize the specimen end to core centroid distance is shown in Figure 3 and is called an H-shaped core. These cores have been made with the web thickness as small as one-tenth millimeter ($\sim 10^{-4} \ell_1$). Assuming (design criterion 2) that one wishes to measure length changes with an accuracy of $3 \times 10^{-8} \ell_1$, and that the "composite specimen" length between core centroids is 0.9999 real specimen and 0.0001 cores, one should either be able to predict the absolute length change of the core material with a maximum error of 1×10^{-4} of the initial core material length and subtract both the initial core web length and its length change, or one should know the relative length change between the specimen material and the core material and subtract this relative length change from the length change measurement.

The H-shaped cores used are machined from Kovar rods and annealed at 1090°C in a H_2 atmosphere for one hour.[9] Since a relatively inaccurate equation of state for Kovar is needed, the room pressure bulk modulus can be used to predict the core length change with sufficient accuracy. The approximation can be improved by making the assumption that the pressure derivative of the bulk modulus is 5.5.

The core web is kept in contact with the specimen end by spring loading with an initial force of 1.4×10^4 dynes (spring compression of 1.3 cm at each specimen end). This spring loading

produces a total end to end specimen strain of 14×10^{-8} cm/cm for an aluminum specimen. Since design criterion 2 suggests length change accuracy of $3 \times 10^{-8}\ \ell_1$, changes in the "spring loading strain" should be corrected for if the latter are of order 10%. The force constant k of the music wire spring changes by 2% in the 8 kbar. pressure range ($\frac{\partial \ell n k}{\partial P} \sim 2 \times 10^{-6}$/bar)[10] and hence will be neglected. However the decreased length of the aluminum specimen combined with the increased length of the pressure vessel at 8 kbar will change each spring compression by about 0.2 cm, which is about 2×10^{-1} of the initial ambient pressure compression. The length change of the pressure vessel and nonmagnetic tails is measured with resistance sensors at each data point. Since the length change of the specimen is measured during each data run, changes in specimen strain caused by spring loading can be predicted within required accuracies.

Phase sensitive detection of the LVDT output (secondary difference voltage) is provided by a highly modified version of a design by Wobschall.[11] This modified design uses a second "reference LVDT" with the same primary current as the "specimen LVDT" and with a fixed position core off null to provide a phase reference used to phase detect the specimen LVDT output. Output sensitivity with H-shaped Kovar cores is shown in Figure 4.

Consider two planes perpendicular to the specimen axis containing the LVDT core centroids and the interferometer mirror reflecting surfaces. These coupling planes are in the center of 2.5 cm thick invar plates (see Figures 5 and 6). The specimen LVDTs are clamped near the bottom of these plates with their axial centers

in the coupling planes. The interferometer mirrors must have two angular degrees of freedom in order to make the two interferometer mirrors approximately parallel and create a fringe pattern. The mechanical arrangement used to allow mirror adjustment while maintaining coupling plane coincidence with the reflecting mirror surface is shown in Figure 6 and consists of a three point spring-loaded support of the interferometer mirror holder. The coupling plate, interferometer mirror holder, and the three support screws are made of Invar with a linear expansion coefficient of 1×10^{-6} cm/cm-°C. Assuming a maximum temperature range of ±10°C and that the maximum coupling error should be $10^{-8}\ \ell_1$, the LVDT core centroid and the interferometer mirror reflecting surface should be coincident with the coupling plane within a total error of 1 mm.

The mechanical configuration used to mount the coupling plate consists of ball bushing shafts and linear adjustable ball bushings. The 3.8 cm diameter ball bushing shafts are supported at three points by aluminum support brackets. All three brackets are clamped to the vessel; however only the center bracket is clamped to the ball bushing shafts to eliminate bending of these rods when the vessel lengthens due to internal pressure. The areas of the vessel in contact with the clamps were ground after heat treatment to insure that the three cylindrical surfaces were on a common support axis.

Three adjustable ball bushings mounted in blocks translate on each shaft. Composite beams made up of an L member and stiffener mount on the ball bushing blocks. These two L member beams-support the two coupling plates and can be independently axially translated to produce LVDT nulls at each end of the specimen. (For details, see

Reference 12).

Since the specimen length change can be as much as 2 cm and the LVDT null sensitivity is about 100 Å, the coupling planes must be capable of translations at least as large as 1 cm with an adjustment capability in the 100 Å range. This is provided by using three modes of translation adjustment in series. Large [(3 cm - .6 mm)/min] and intermediate [(.3 mm - 10^3 Å)/sec] translations are provided by motor driven micrometers. Small translations ($\sim 10^4$ Å with $<$100 Å adjustment capability) are produced by ceramic piezoelectric wafers.

These three translation production devices are mounted in a translation stage which provides relative motion between a ball mounted on the L member stiffener and the aluminum oil bath frame.

Design criterion 2 requires reference length stability of about 1×10^{-8} cm/cm. Therefore the helium-neon single mode laser (Spectra Physics 119) used to generate the interferometer wavelength must be referenced to the center of the Lamb dip[13], and the interferometer path length index of refraction should be stabilized or known to better than 1×10^{-8}. The block diagram of the interferometer system is shown in Figure 7. The laser output wavelength is manually adjusted to better than 1×10^{-8} Å/Å of the Lamb dip minimum for each data point by modulating the laser wavelength by $\pm 1.5 \times 10^{-7}$ Å/Å and displaying laser power (vertical) versus modulation signal (horizontal) on an X-Y oscilloscope.[14] This technique avoids uncertainty due to Lamb dip distortion caused by optical feedback from the interferometer to the laser. The interferometer path is kept at a pressure of the order of tens of microns. This pressure is

recorded for each data point, and corrections are applied for the effect on the interferometer wavelength of the non-zero pressure. In order to minimize thermal and vibrational coupling to the experiment, the vacuum system is pumped down to about 1 micron and then is isolated before a data run is started.

The interferometer beam diameter of 4 mm is defined by the laser output telescope and the beam divergence (0.2 milliradians). The interferometer beams reflected from mirror B and mirror A (see Figure 7) combine into a fringe pattern beam which is reflected from the beam splitter and passes through a divergent lens, resulting in a fringe pattern image diameter near to 20 mm. The fringe spacing f_s ranges from 0.0 mm (optics not aligned) to a maximum spacing of about 3 mm. The adjustable beam splitter mount translates the fringe pattern relative to two solid state photodiodes (Hewlett-Packard Model 4205), mounted with a center to center distance of 2.5 mm. The small optically active diameter (0.6 mm including lens effect) and small optical acceptance angle (near $\pm 20°$ from optic axis of diode) eliminate the need for slit arrangments and shielding from room lights when the thermal insulation is removed.

The two photodetector amplifier outputs act as inputs to both a reversible counter and an X-Y oscilloscope equipped with a polar coordinate graticule which allows measurement of the fringe motion to 1/40 of the fringe spacing. The integral part of the fringe count output, representing one-quarter fringes, is read from the nixie-tube output of the reversible counter, and the decimal interpolation is read from the location of the fringe trace on the polar coordinates of the oscilloscope graticule.

The coarse motion rate of the remote translation control (0.6 mm/min) corresponds to about 35 fringes/sec. However, the frequency response of the photodetector amplifiers and reversible counter system should be much higher than 35 hz to allow for vibration and shock induced motion. The photodetector amplifiers have a high frequency cutoff of 70 khz. The high frequency cutoff for the oscilloscope and counter inputs has been lowered to 0.5 khz to avoid counting electrical transients. This 0.5 khz frequency response has been adequate to handle shock (from slamming doors, jumping on floor, pounding fist on table, etc.) and vibration (typically less than 100 hz) induced fringe motion.

Measurement of initial specimen length

The initial specimen length ($\ell_1(T_1,P_1)$) measurement technique uses an intermediate reference length which is located parallel to the specimen axis. One end of the intermediate reference length is magnetically clamped to an invar coupling plate. The second end has an attached LVDT core located on the axis of an LVDT mounted in the second invar coupling plate. This intermediate reference length can be left in position all the time, while either a standard length or a specimen is placed on the specimen axis. An $\ell_1(T_1,P_1)$ measurement proceeds as follows:

(1) Position a standard length with a known distance between LVDT core centroids in place of the specimen.

(2) Translate both coupling planes to produce LVDT nulls at each end of the standard length.

(3) Translate one coupling plane to produce an LVDT null on the intermediate reference length core, using the

interferometer to measure this displacement.

(4) Replace the standard length with the specimen and its LVDT cores and produce the T_1, P_1 specimen environment (without worrying about disturbing the interferometer fringe count--indeed weeks could elapse between steps 1 to 3 and step 5).

(5) Proceed backwards through steps 1 to 3, resulting in a measurement of the difference in length between the specimen and the standard (known) length, and hence ℓ_1.

The ℓ_1 measurement error is principally limited by the length stability of the standard length and the intermediate reference length, and the error in measuring the core centroid to core centroid distance of the standard length.

Temperature Control and Measurement

The 1 meter long specimen is located on the axis of the pressure vessel, partially thermally isolated from an oil bath by the pressure medium, the maraging steel pressure vessel, and the thermal interfaces of the vessel with the pressure medium and the vessel surroundings. The thermal time constant between the specimen and the oil bath is 28 minutes, resulting in a thermal filtering of rapid oil bath temperature changes. Although some "A.C." may be present in the oil bath temperature, the "D.C." level must be maintained to accuracies or nearly 1 m°C for periods of about one week to maintain the desired specimen temperature stability.

The design chosen to satisfy these requirements was a recirculating oil bath where the thermal inputs of heater power and viscous heating are balanced by a cooling heat exchanger and

ambient leakage, resulting in an adiabatic oil flow. See Figure 8. Temperature control is achieved by sensing oil temperature as oil enters the bath and proportionally controlling the heater power to maintain constant oil temperature.

A typical thermal balance is:

Heater Power	P_H = + 16 watts
Viscous Heating Power	P_V = + 47 watts
Ambient Leakage Power	P_L = - 25 watts
Cooler Power	P_C = - 38 watts

where $P_H + P_V + P_L + P_C = 0$ watts, the total thermal wattage to the oil.

The temperature control of the oil at the sensing point can only be as stable in time as the temperature sensor stability. Since the design criteria call for long term (1 week) stability of 1 m°C, platinum resistance temperature sensors were used.[15]

A temperature sensitive bridge[12] using two platinum sensors (Rosemount-Model 134MA-16) and two low temperature coefficient switch selected resistors is used to control the oil heater power. The switch selectable null temperatures ranges from 27°C to 55°C in steps of about 0.25°C. Separate platinum sensors located in the oil bath near each end of the pressure vessel are used to measure the specimen temperature. The cooling water and ambient air are temperature controlled to accuracies of ±0.05°C and ±0.2°C respectively.

DISCUSSION OF RESULTS

Two length measurements are used to define the relative length $\frac{\ell_1}{\ell}$; one is the specimen length change $\Delta\ell(T,P)$, the other is the initial specimen length measurement $\ell_1(T_1,P_1)$. The largest contribution to an ℓ_1 error is the uncertainty in absolute length of the standard length rods and time stability of the reference length rod. These effects create an uncertainty of about $\pm 1.5 \times 10^{-5}\ \ell_1$ in the ℓ_1 measurment, contributing a systematic error to ℓ_1/ℓ of about $\pm 1.5 \times 10^{-5}$. However, since we are interested in relative changes in ℓ_1/ℓ, this systematic error is not serious.

The $\Delta\ell(T,P)$ measurement includes both systematic and random sources of error. Assuming that the random sources of error are pressure and temperature independent, random effects can be evaluated by replication of a number of measurements during a length stability run at constant pressure and temperature. Including as random error sources nulling both LVDTs, translating both coupling planes, random interferometer errors, and average specimen temperature fluctuations, the standard deviation $\sigma_{\Delta\ell}$ has been measured by monitoring the specimen length every 20 minutes for a period of 24 hours using the LVDTs, the interferometer, the temperature control system, and moving each coupling plane (at least 10^3 counts) before each measurement. The standard deviation of the 73 measurements is $\sigma_{\Delta\ell} = 1.9 \times 10^{-8}\ \ell_1$ (pressure and temperature equivalents for this strain of an aluminum specimen are 0.04 bar or 0.8m°C). A systematic difference of $4 \times 10^{-8}\ \ell_1$ was observed between data points taken after the coupling planes were translated toward each other

and after the coupling planes were translated away from each other. Because of this hysteresis, all data points have been taken after the coupling planes have been translated toward each other by at least 10^3 counts.

Now consider possible sources of systematic error in the $\Delta\ell(T,P)$ measurement. Three of these have been discussed previously. They are the LVDT core length correction, the spring loading length correction, and the vacuum leak correction to the laser wavelength. These systematic errors have predictable effects on $\Delta\ell(T,P)$, and appropriate corrections have been applied.

The least well evaluated possible systematic error in the length change measurement is due to a possible systematic tilting of the coupling planes as the coupling planes are translated along the specimen axis. This possible systematic error can at least be bounded by considering the effect of a rotation of a coupling plate (and interferometer reflector) on the observed fringe pattern. Observing that translating the coupling plates 5 cm (which is greater than 15 times the maximum $\Delta\ell$ for $P_{max} \leq 8$ kbar and $B_T \geq 800$ kbar) produces less of an effect on the fringe circle than 0.1 of a turn of the mirror angular adjustment knob and that 0.1 of a turn corresponds to nearly 2×10^{-5} radians of angular mirror motion, the systematic coupling plane rotation error is less than $2\times10^{-6}\ \ell_1$ for $\Delta\ell$ = 5 cm. For a reasonable $\Delta\ell$ (0.3 cm for aluminum) the possible systematic error limit should be less than $2\times10^{-7}\ \ell_1$. A design modification that would eliminate this possible systematic error would be to use a "double interferometer configuration", with laser beams equally spaced above and below the specimen axis.

In this case tilting of the coupling planes would lengthen one beam and shorten the other. The specimen length change would be calculated from the average fringe count change of the two interferometers.

Figure 9 shows the approach to equilibrium after a pressure change from near 1.5 kbar to near 2.0 kbar. The dotted line shows the (manganin gauge) measured pressure (relative to equilibrium) as a function of time. The dashed line represents a calculated specimen length approach to equilibrium assuming that the specimen temperature is constant and the specimen length is only a function of the measured pressure. The solid line represents the measured specimen length as it approaches equilibrium.

The difference in strain between the solid line and the dashed line represents the specimen strain due to the temperature transient associated with the partly adiabatic compression of the hexane. This strain is about 2.3×10^{-7} cm/cm approximately 30 minutes after the pressure change, implying a 10 m°C thermal effect approximately 30 minutes after the pressure change. During a length versus pressure measurement at constant temperature the approach to equilibrium is monitored at about 15 minute intervals with the final data usually taken over 2 hours after the pressure change.

A stability run at 5 kbars was designed to measure the pressure loss rate due to leaks in the pressure system. No pressure loss was noticeable in a 24 hour period, implying a pressure loss rate less than 0.2 bar/day at 5 kbars.

At the present time Al (polycrystalline, commercial alloy 6061-T6) and Si (single crystal, resistivity $\sim$1 Ω-cm) have been used as specimens. The aluminum specimen, chosen primarily for

its high thermal expansion coefficient, demonstrated the average specimen temperature stability achieved, but suffered from length hysteresis with pressure cycling. Length change data was taken in the pressure range of 0.001 to 5 kbar; specimen length hysteresis of about $-4\times10^{-6}\ \ell_1$ was observed (the negative sign indicates that the specimen length was shorter after the pressure cycle). The specimen was exposed five times to 7.3 kbar and again length change data was taken in the 0.001 to 5 kbar range. The specimen length hysteresis decreased to $-1\times10^{-6}\ \ell_1$.

After considering a model of spherical voids in an infinite sphere subjected to a pressure P, and noting that plastic yielding occurs for $P > \frac{2}{3}\sigma_o$, where σ_o is the yield stress of the solid (about 3 kbars for this aluminum alloy), pressure runs were limited to P_{max} = 2 kbars. Length change data was taken in the pressure range of 0.001 to 2 kbar, resulting in a specimen length hysteresis of $+1\times10^{-7}\ \ell_1$.

It was felt that the 0-2 kbar aluminum hysteresis might be due to dislocation generation near elastic inhomogenities (grain boundaries or precipitated second phase). A 106 cm long single crystal of Si (purchased from Texas Instruments, Inc.) was spark cut and chemically etched to the appropriate specimen geometery. Length change data taken in the pressure range 0.001 to 7.5 kbar and then curve fit to expected functional forms indicates that the initial atmospheric data point is typically in error by $1\times10^{-7}\ \ell_1$, with the approximately 15 remaining data points having a standard error of $3\times10^{-8}\ \ell_1$ from the two or three adjustable parameter functional form.

Further discussion of the Si results will be given in a subsequent paper.

Using the manganin gauge calibrated by Ruoff, Lincoln and Chen,[2] we obtained from the present length measurement an isothermal bulk modulus of polycrystalline 6061-T6 aluminum at zero pressure of B_o^T = 0.7248 ± 0.001 Mbars and the pressure derivative of $B_o^{T'}$ = 4.77 ± 0.08. This is to be compared with the values of 0.7292 ± 0.0010 Mbars and 5.15 ± 0.14 obtained ultrasonically by Ho and Ruoff[16] on single pure crystals and of 0.717 Mbars and 4.96 obtained by Ho and Ruoff[16] from the shock data of Munson and Barker[17] on polycrystalline 6061-T6 aluminum.

ACKNOWLEDGEMENTS

We would like to thank Robert E. Terry, whose technical assistance made this apparatus possible. We are indebted to Tom Seddon for his work on nonlinear curve fitting. We appreciate the comments made by Prof. Ralph Simmons on our length measurement design. We want to thank P. B. Ghate and Martin Jones for their help in procuring the silicon crystals from Texas Instruments and B. Addis for his help in machining them to their final dimensions. We appreciate the effort made by Joseph Lipschutz of Schaevitz Engineering in designing the special LVDT configuration. We appreciate the help of Universal Instruments in absolute length mensuration. We acknowledge the support of this work by the United States Atomic Energy Commission under Contract AT (11-1) 3153 and the Advanced Research Projects Agency and the National Science Foundation for support of facilities of the Cornell Materials Science Center used in this work.

REFERENCES

1. W. C. Overton, Jr. J. Chem. Phys. 37, 116 (1962).
2. Arthur L. Ruoff, R. C. Lincoln and Y. C. Chen, United States Atomic Energy Report COO-2504-98, submitted for publication.
3. P. W. Bridgman, Proc. Am. Acad. Arts. Sci. 77, 189 (1949).
4. P. W. Bridgman, Proc. Am. Acad. Arts Sci. 74, 11 (1940).
5. C. A. Rotter and C. S. Smith, J. Phys. and Chem. Sol. 27, 267 (1966).
6. H. Ebert, Phys. Z. 36, 391 (1935).
7. A. H. Smith, N. A. Riley, and A. W. Lawson, Rev. Sci. Instr. 22, 138 (1951).
8. J. Reitzel, I. Simon, and J. A. Walker, Rev. Sci. Instr. 28, 828 (1957).
9. Private communication, J. Lipshutz, Schaevitz Engineering, Camden, N.J.
10. R. H. Cornish, Ph.D. Thesis, Cornell University, Ithaca, New York (1962).
11. D. Wobschall, Rev. Sci. Instr. 32, 71 (1961).
12. R. C. Lincoln, Ph.D. Thesis, Cornell University, Ithaca, New York (1971).
13. W. E. Lamb, Jr., Phys. Rev. 134, 1429 (1964).
14. For example, see "Stable Laser Application Note 1," Electro Optics Associates (Palo Alto, Calif.) or "Model 119 Gas Laser Operation and Maintenance Manual," Spectra-Physics, Inc. (Mountain View, Calif.).
15. For example, see Herzfeld, "Temperature - Its Measurement and Control in Science and Industry - Volume 3 - Part 1" [Reinhold Publishing Co., New York (1962)], page 310; or Kutz, "Temperature Control" [John Wiley and Sons, New York (1968)] Chapter 6.6.
16. P. S. Ho and A. L. Ruoff, J. Appl. Phys. 40, 3151 (1969).
17. D. E. Munson and L. M. Barker, J. Appl. Phys. 37, 1652 (1966).

FIGURE LEGENDS

Figure 1: Schematic of length measurement system.

1) Laser path vacuum bellows.
2) Laser beams.
3) Interferometer mirrors.
4) Coupling plates. Mirrors and LVDT's are mounted on these plates which move longitudinally on two longitudinal shafts located behind and in front of pressure vessel.
5) LVDT's.
6) Pressure vessel (schematic). Actually the magnetic core is located within nonmagnetic "tails" of reduced diameter on the ends of the vessel.
7) Specimen (schematic).
8) LVDT cores.

Figure 2: Assembly view of nonmagnetic tail with LVDT and portion of specimen.

1) Specimen.
2) Ball bushing support for specimen.
3) Portion of specimen supported by ball bushing.
4) Bridgman seal-mushroom.
5) Bridgman seal - Indium ring.
6) Bridgman seal - Miter ring (one of four).
7) Bridgman seal - Thrust collar.
8) Bridgman seal - Thrust nut.
9) Bridgman stem - (12.7 mm O.D. by 5.6 mm I.D. - 316 stainless steel high pressure tubing).
10) Bridgman seal - Extractor clamp.
11) Linear variable differential transformer (LVDT).
12) LVDT positioning ball.
13) LVDT core ("H" shape core).
14) LVDT core retaining spring.
15) Gland nut for connector.
16) Tuning collar for connector.
17) Tubing connector.
18) End plug.

Figure 3: H-shaped core.

Figure 4: Displacement coupling sensitivity with H-shaped Kovar core located on the axis of 12.7 mm O.D. by 5.6 mm I.D. stainless steel tubing with LVDT outside the tubing.

Figure 5: Partial side view of coupling plate (one of two shafts on which plate moves along axis of specimen is shown as item 9 in Figure 6).

Figure 6: Photograph of coupling plate.

1) "L" member.
2) "L" member stiffener.
3) Nonmagnetic tail.
4) Specimen LVDT.
5) Coupling plate.
6) Mirror angular adjustment knobs.
7) Mirror angular adjustment screws.
8) Ball bushing shaft support.
9) Ball bushing shaft.
10) Ball bushing block.

Figure 7: Interferometer system.

Figure 8: Temperature control system.

Figure 9: Approach to equilibrium after a pressure change. The difference between the dashed line (calculated specimen strain due only to the observed pressure transient) and the solid line (observed specimen strain) represents the specimen strain caused by the temperature transient associated with the sudden 1.5 kbar to 2.0 kbar pressure change.

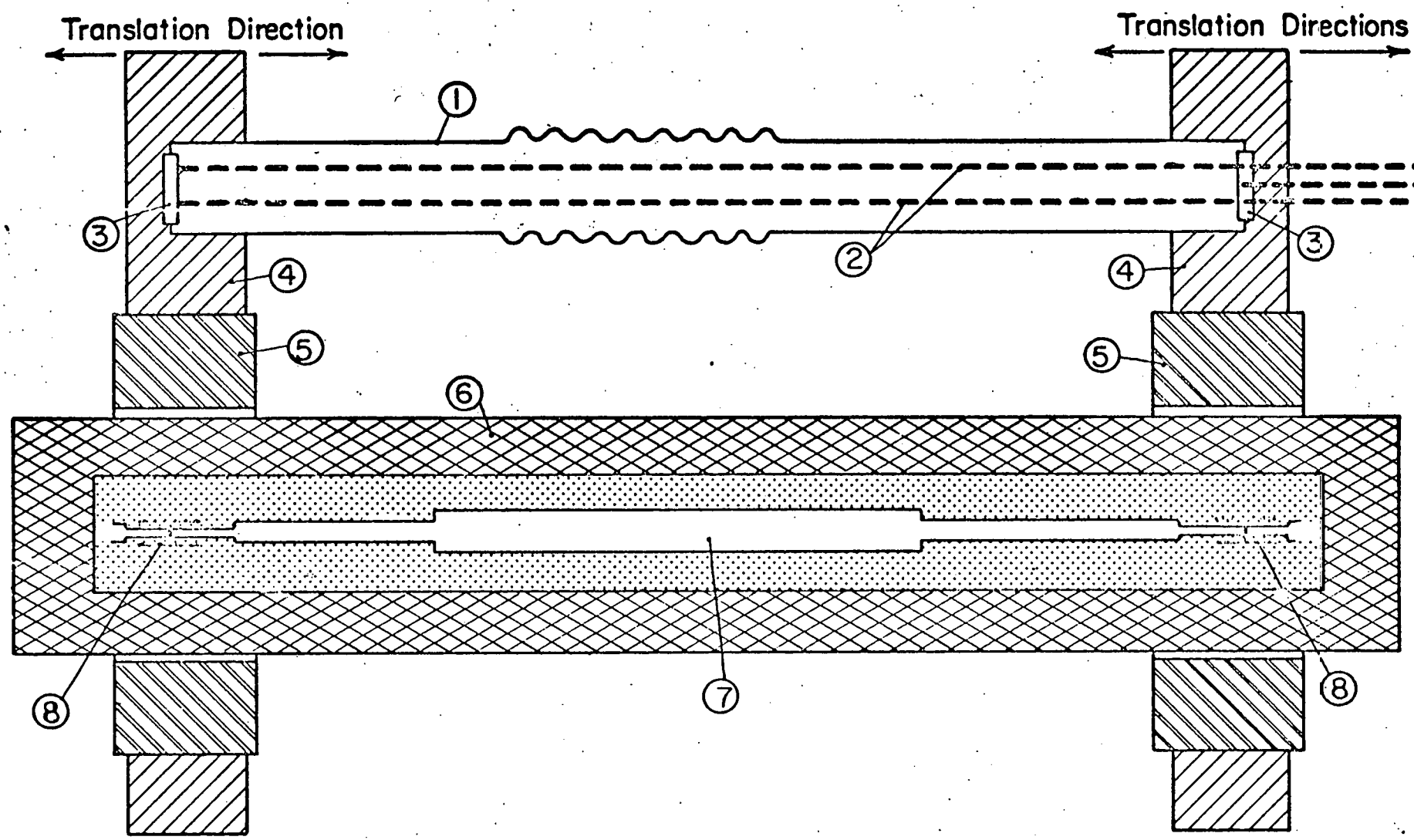
Translation Direction
Translation Directions
1
2
3
3
4
4
5
5
6
7
8
8

Fig. 1

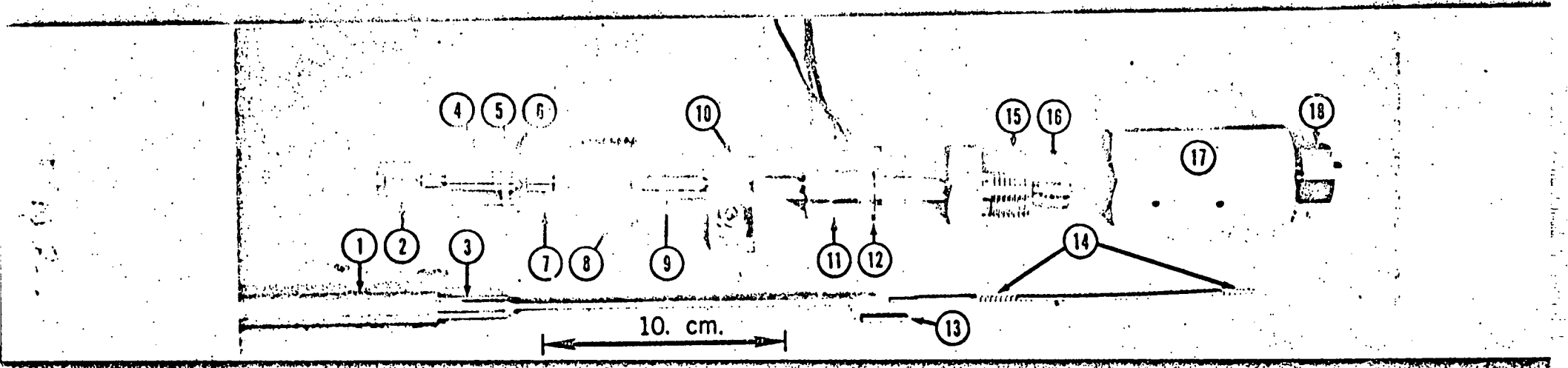
4
5
6
10
15
16
18
17
1
2
3
7
8
9
11
12
14
13
10. cm.

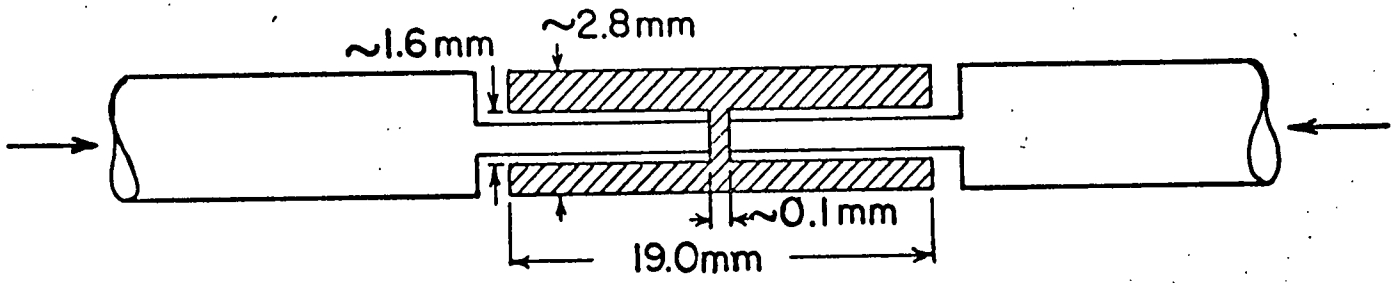

"H" shape core.
Core length change correction known and small. Requires spring loading.

 Indicates magnetically soft ferromagnetic material.

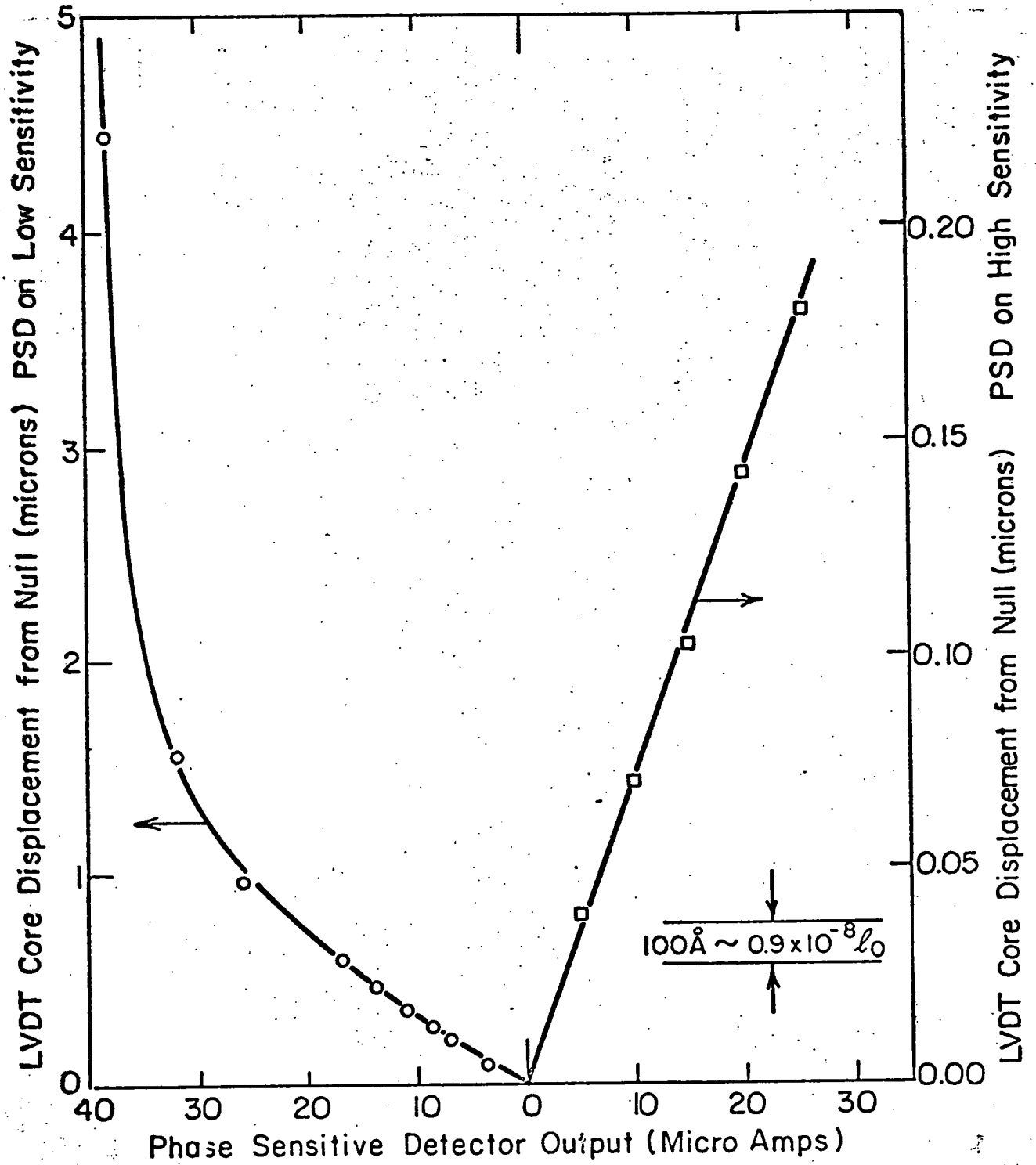
LVDT Core Displacement from Null (microns) PSD on Low Sensitivity
LVDT Core Displacement from Null (microns) PSD on High Sensitivity
Phase Sensitive Detector Output (Micro Amps)
0
1
2
3
4
5
0.00
0.05
0.10
0.15
0.20
40
30
20
10
0
10
20
30
100Å ~ 0.9x10⁻⁸ℓ₀

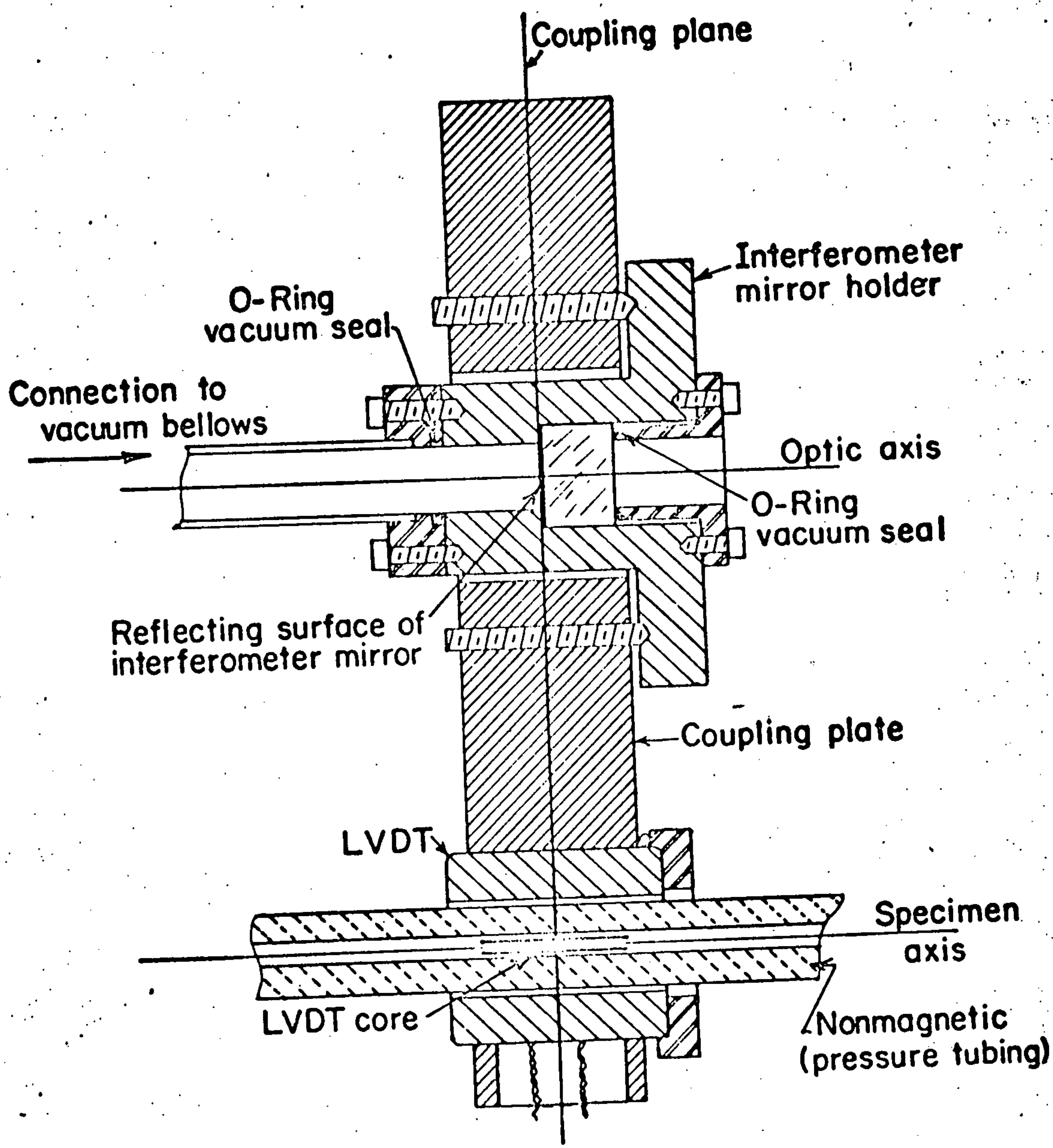
Coupling plane
Interferometer
mirror holder
O-Ring
vacuum seal
Connection to
vacuum bellows
Optic axis
O-Ring
vacuum seal
Reflecting surface of
interferometer mirror
Coupling plate
LVDT
Specimen
axis
LVDT core
Nonmagnetic
(pressure tubing)

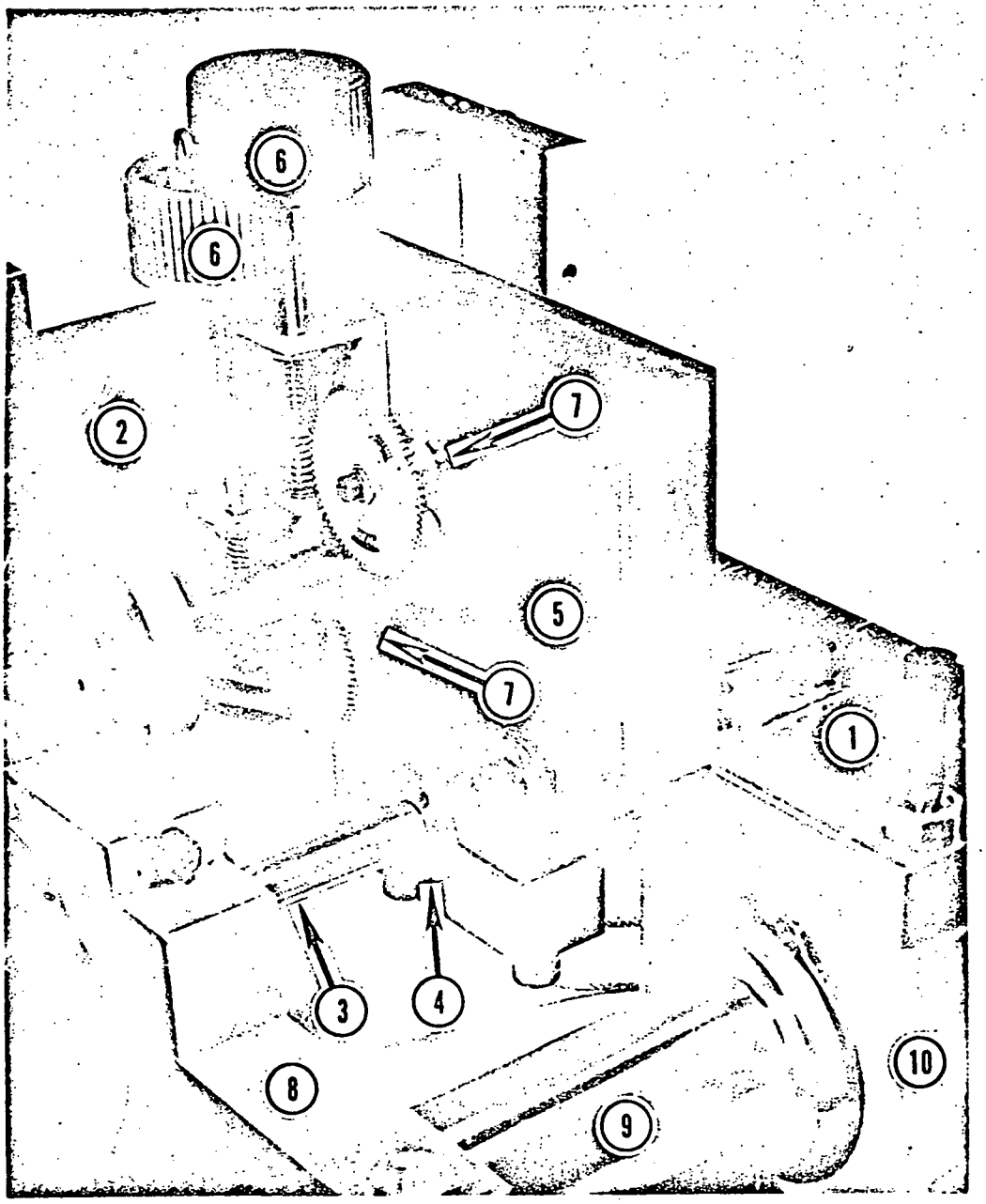

Fig 6

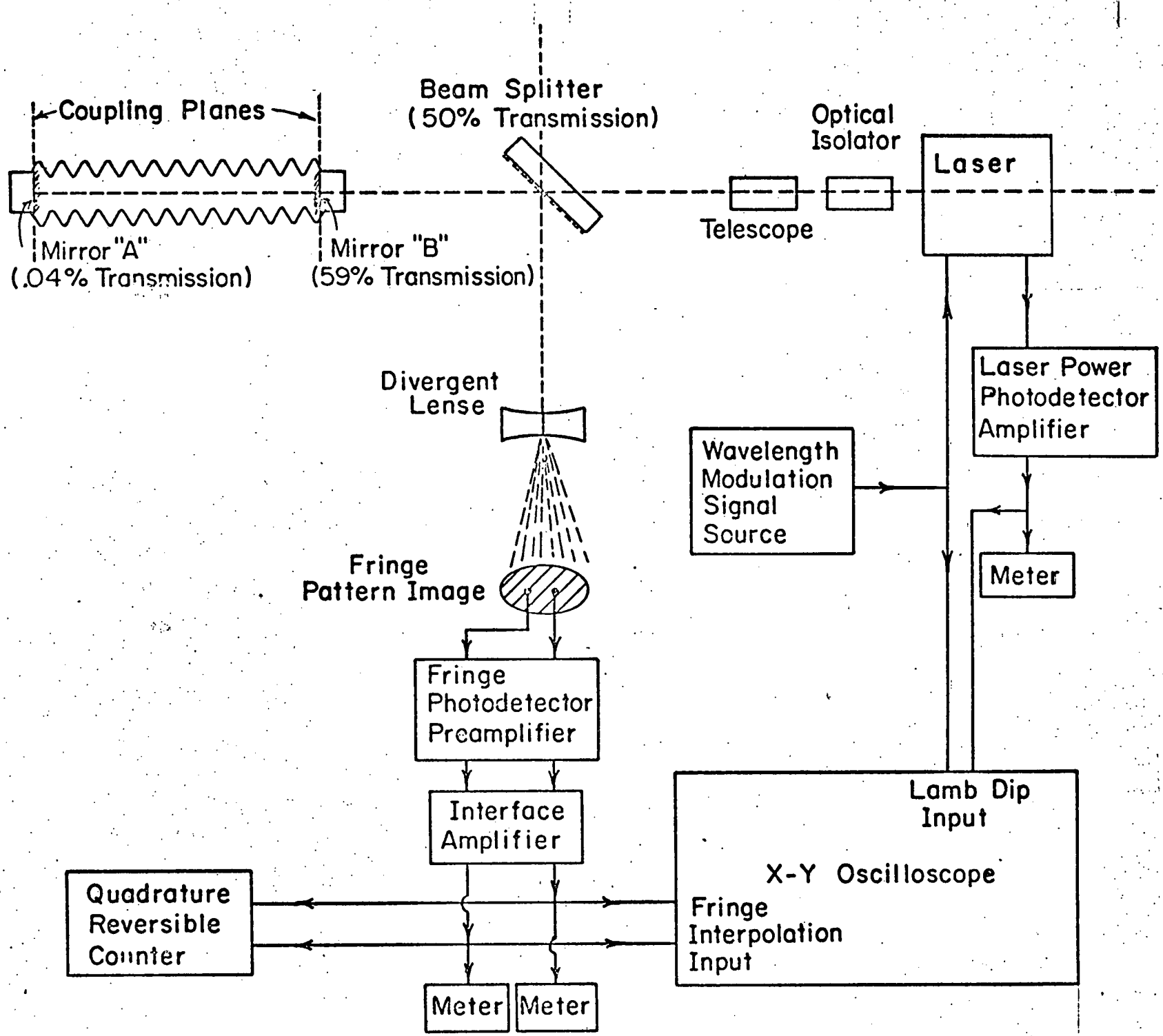
Coupling Planes
Beam Splitter
(50% Transmission)
Optical
Isolator
Laser
Telescope
Mirror "A"
(.04% Transmission)
Mirror "B"
(59% Transmission)
Divergent
Lense
Laser Power
Photodetector
Amplifier
Wavelength
Modulation
Signal
Source
Meter
Fringe
Pattern Image
Fringe
Photodetector
Preamplifier
Interface
Amplifier
Lamb Dip
Input
X-Y Oscilloscope
Quadrature
Reversible
Counter
Fringe
Interpolation
Input
Meter
Meter

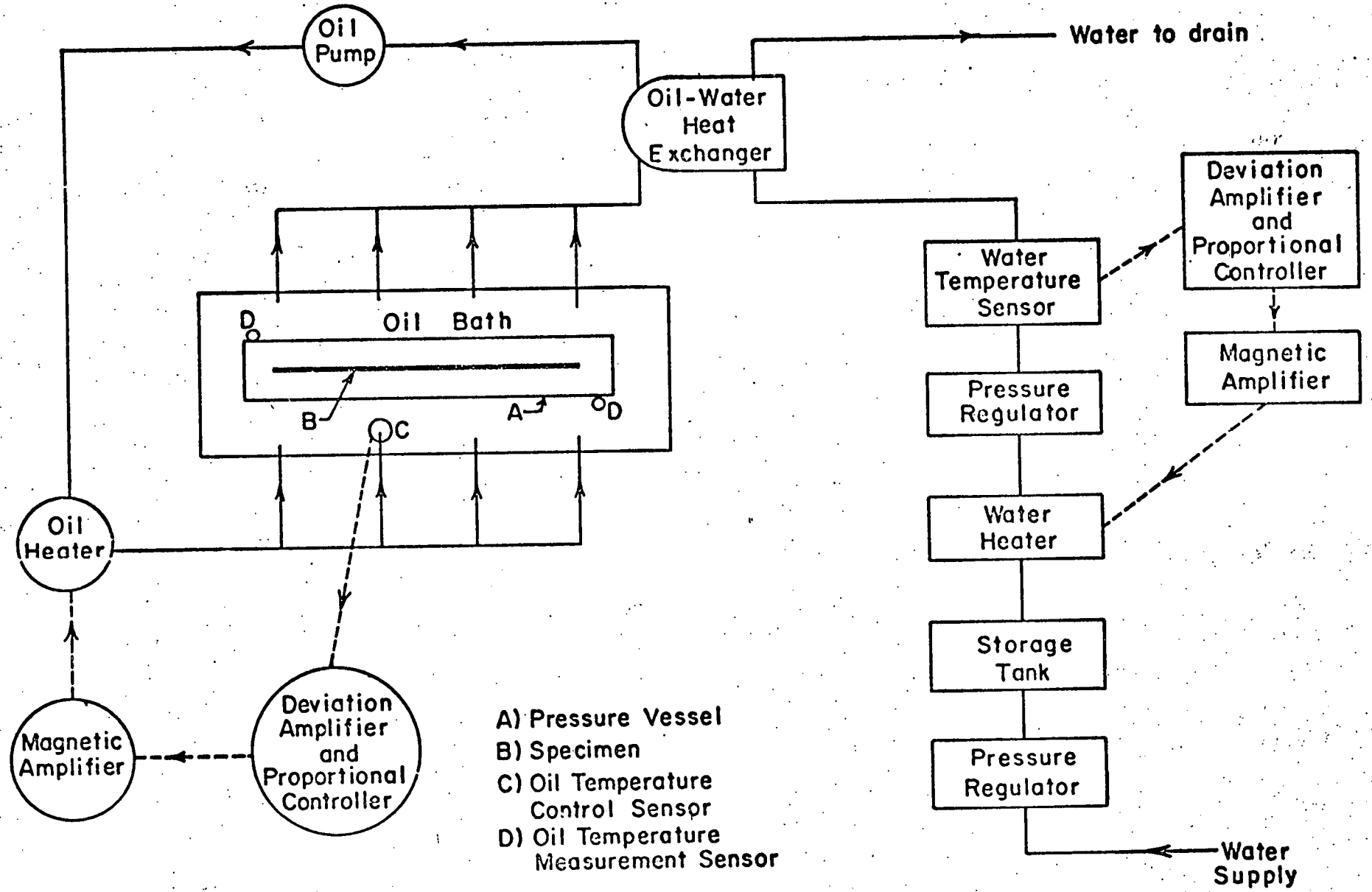
Oil Pump
Water to drain
Oil-Water Heat Exchanger
Deviation Amplifier and Proportional Controller
Water Temperature Sensor
Oil Bath
D
B
A
D
C
Magnetic Amplifier
Pressure Regulator
Oil Heater
Water Heater
Storage Tank
Pressure Regulator
Water Supply
Magnetic Amplifier
Deviation Amplifier and Proportional Controller
A) Pressure Vessel
B) Specimen
C) Oil Temperature Control Sensor
D) Oil Temperature Measurement Sensor

Fig. 6

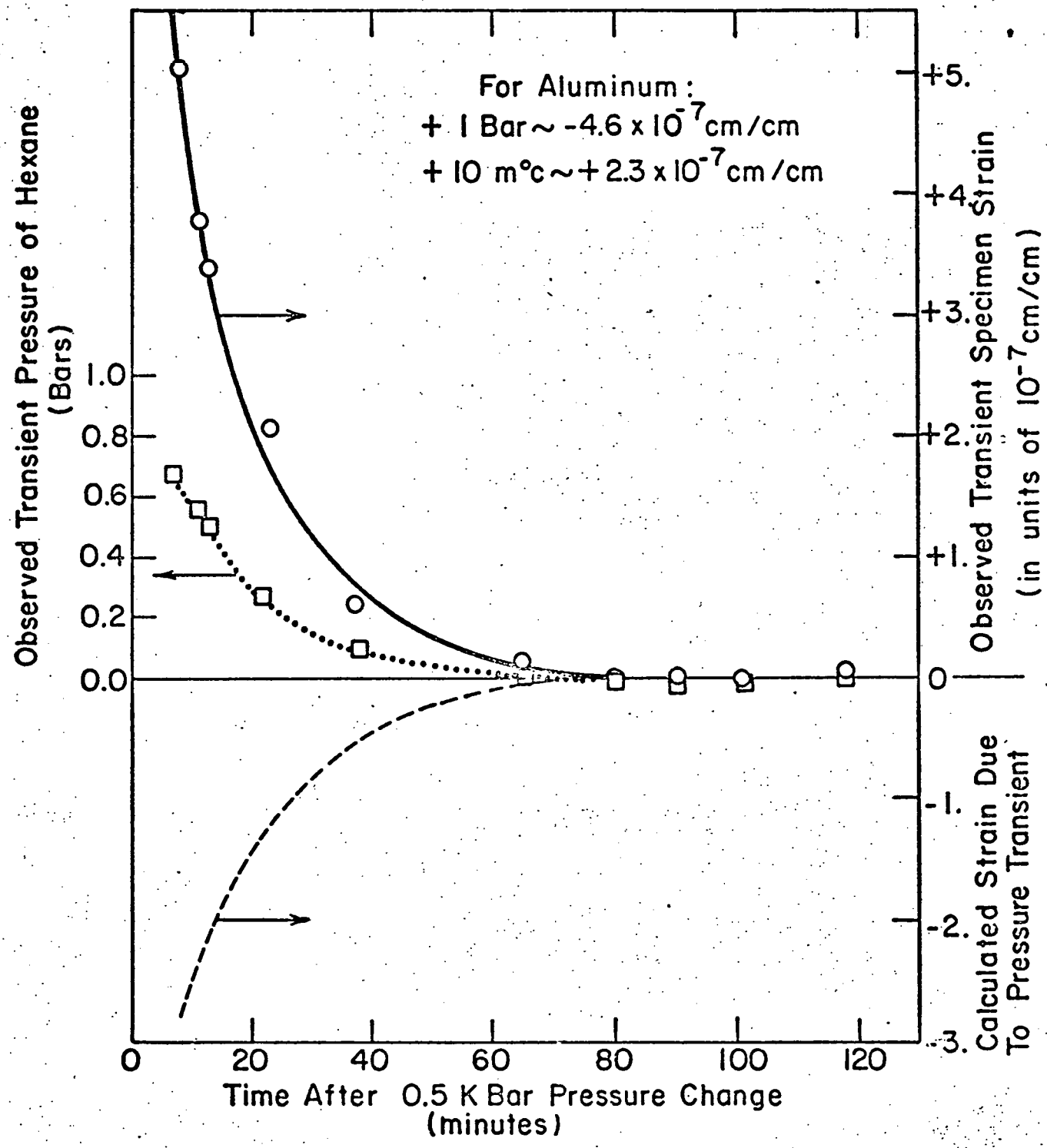
For Aluminum:
+ 1 Bar ~ -4.6 x 10^-7 cm/cm
+ 10 m°c ~ +2.3 x 10^-7 cm/cm
Observed Transient Pressure of Hexane (Bars)
1.0
0.8
0.6
0.4
0.2
0.0
+5.
+4.
+3.
+2.
+1.
0
-1.
-2.
-3.
Observed Transient Specimen Strain (in units of 10^-7 cm/cm)
Calculated Strain Due To Pressure Transient
0
20
40
60
80
100
120
Time After 0.5 K Bar Pressure Change (minutes)

Fig. 9